J. Chem. Sci. (2018) 130:114
https://doi.org/10.1007/s12039-018-1521-5

REGULAR ARTICLE

Synthesis, characterization, spectroscopy and biological activity of 4-((3-formyl-4-hydroxyphenyl)azo)-1-alkylpyridinium salts

SAKINEH OMIDI[a], VIDA KHOJASTEH[a], ALI KAKANEJADIFARD[a,*], MOTALEB GHASEMIAN[a] and FARIDEH AZARBANI[b]

[a]Department of Chemistry, Faculty of Science, Lorestan University, Khorramabad, Iran
[b]Department of Biology, Faculty of Science, Lorestan University, Khorramabad, Iran
E-mail: ali.kakanejadifard@gmail.com; kakanejadi.a@lu.ac.ir

MS received 30 December 2017; revised 24 April 2018; accepted 20 June 2018; published online 2 August 2018

Abstract. The reaction of 2-hydroxy-5-(pyridine-4-yldiazenyl)benzaldehyde with n-alkyl bromides generated five novel azo pyridinium salts in good to excellent yields. The ^{1}H and ^{13}C NMR and UV-Vis absorption spectra indicated several tautomers for the new compounds. The NMR, UV-Vis absorption spectra and quantum chemical calculations show that the azo pyridinium salts have a new resonant structure compared to the corresponding azo precursor. Antibacterial activity was studied by disc diffusion and MIC methods. Diphenylpicrylhydrazyl (DPPH) assay was used to determine the antioxidant properties. The effects of carbon chain length on antimicrobial activity were also investigated. The results showed that existence of alkyl groups is crucial for the antibacterial properties. The new compound with decyl group displayed the best antibacterial activity.

Keywords. Azo compounds; pyridinium quaternary salts; antibacterial activity; theoretical study.

1. Introduction

Azo compounds cover a major portion of industrial dyes, as aromatic azo compounds are largely colored.[1–3] The rich chemistry of azo compounds is related to several important biological properties such as antibacterial, antifungal, antitumor and antioxidant activities.[4–6] Also, azo compounds are utilized as therapeutic agents and can be used to image amyloid plaques in the brains of Alzheimer's patients.[7]

Some azo dyes are also applied in drugs and cosmetics.[8] Azobenzenes display a reversible isomerization between trans and cis isomers by diverse stability and this feature is used in the development of photomechanical processes and medical fields.[9–11] Heterocyclic moieties, such as pyridine have been utilized for the synthesis of new azo dyes to enhance their color strength and brilliant shades.[12,13] Azo pyridine derivatives have a wide range of biological activities. For example, phenazopyridine, with the trade name of 'pyridium', is used as a urinary analgesic.[14]

Long alkyl chain quaternary ammonium compounds (QACs) exert a broad range of antibacterial activity against Gram-positive and Gram-negative bacteria, some pathogenic species of fungi and protozoa.[15,16] The amphiphilic nature of QACs, are concurrently exploited for their surfactant, preserving and antimicrobial properties in some cosmetic and personal care products.[17,18] Structural aspects and a variety of biological activities of azo compounds and quaternary pyridinium salts were a motivation for the synthesis of five new azo compounds containing long chain alkyl pyridinium salts for the studies of antibacterial and antioxidant properties.

2. Experimental

2.1 *Materials and measurements*

All the chemicals, reagents, and solvents were purchased from Merck (Germany) and used without further purification. The solvents used in the reactions were analytically reagent grade. 2-Hydroxy-5-(pyridine-4-yldiazenyl)benzaldehyde (**1**) was

*For correspondence

Electronic supplementary material: The online version of this article (https://doi.org/10.1007/s12039-018-1521-5) contains supplementary material, which is available to authorized users.

prepared and purified according to the method reported in the literature.[19] Melting points were measured on an Electrothermal 9200 apparatus. Mass spectra were recorded on an Agilent MS Model 5973. FT-IR spectra were recorded on a Shimadzu 8400S spectrometer using KBr disc. The electronic absorption spectra were recorded with a Shimadzu 1650 spectrophotometer. ^{1}H and ^{13}C NMR spectra were recorded in DMSO-d_6 as the solvent on the Bruker DRX-300 MHz and 400 MHz Advance spectrometers.

2.2 *General procedure for the synthesis of 4-((3-formyl-4-hydroxyphenyl)azo)-1-alkylpyridinium bromide (***2a–e***)*

To a stirring solution of 2-hydroxy-5-(pyridine-4-yldiazenyl) benzaldehyde (**1**, 10 mmol, 2.27 g) in ethanol (200 mL), was added the relevant alkyl bromide (12 mmol) at 78 °C. The mixture was stirred and refluxed for 24 h, and the solvent was removed. The resultant solid material was collected and washed with cold diethyl ether and dried. The products are soluble in acetonitrile dimethylsulfoxide (DMSO), *N*,*N*′-dimethylformamide (DMF), methanol (CH_3OH), ethanol (C_2H_5OH), (CH_3CN) and tetrahydrofuran (THF), (see Supplementary Information).

2.3 *Compound 4-((3-formyl-4-hydroxyphenyl)azo)-1-methylpyridinium iodide (***2a***)*

Maroon solid. Yield: 88%; M.p.: 242–244 °C. IR (cm^{-1}): νOH 3475, $\nu CH_{aliphatic}$ 2920, νCH=O 2736, νC=O 1654, νN=N 1600, νC=C 1488, νC-O 1278; ^{1}H NMR (δ, ppm in DMSO-d6): 10.39-10.19 (s,1H, C<u>H</u>O), 8.78 and 8.56, 8.54 (d, 2H, *J*/Hz 6.60), 8.21, 8.20 and 7.80, 7.99 (d, 1H, *J*/Hz 2.43), 8.12, 8.11, 8.09, 8.08 and 7.88, 7.87, 7.85, 7.84 (dd, 1H, ^{3}J/Hz 9.71, ^{5}J/Hz 2.46), 7.81, 7.79 and 7.71 (d, 2H, *J*/Hz 6.63), 7.18, 7.15 and 6.41, 6.38 (d, 1H, *J*/Hz 9.72), 4.11 and 3.66 (s, 3H); ^{13}C NMR (δ, ppm in DMSO-d6): 190.72 and 190.26, 182.96, 165.27, 162.06, 145.10, 144.33, 141.48, 129.84, 127.52, 126.20, 125.18, 122.80, 119.03, 116.19 and 45.75 (CH_3); HR-MS (EI-MS) m/z calc. for $C_{13}H_{12}IN_3O_2$ $(M+H+18)^+$ 388.17, found 388.3 and HR-MS (EI-MS) m/z calc. for $C_{13}H_{11}N_3O_2$ $(M-H-I)^+$ 241.25, found 241.4.

2.3a *Compound 4-((3-formyl-4-hydroxyphenyl)azo)-1-decylpyridinium bromide (***2b***)*: Dark brown solid. Yield: 89%; M.p.: 265 °C. IR (cm^{-1}): νOH 3432, $\nu CH_{aliphatic}$ 2925, 2854, νCH=O 2736, 2854, νC=O 1663, νN=N 1594, νC=C 1484, νC-O. 1267; ^{1}H NMR (δ, ppm in DMSO-d6): 10.38–10.10 (s,1H, C<u>H</u>O), 8.75–8.65 (bs, 2H), 8.01, 8.00 (d, 1H, *J*/Hz 2.16), 7.87, 7.85, 7.80, 7.79 (dd, 1H, ^{3}J/Hz 9.34, ^{5}J/Hz 2.17), 7.55 (d, 2H); 6.57, 6.54 (d, 1H, *J*/Hz 9.3), 4.33 and 4.15 (t, 2H); 1.78–1.72 (m, 2H), 1.36–1.12 (bs, 14H), 0.76 (t, 3H); ^{13}C NMR (δ, ppm in DMSO-d6): 191.20, 183.34, 177.66, 162.34, 157.58, 151.52, 151.02, 144.41, 141.64, 139.57, 133.25, 127.80, 126.82, 126.32, 125.24, 123.74, 116.62, 115.61, 31.36, 30.67, 28,94, 28.74, 28.50, 25.53, 22.182, 22.182 and 14.03; HR-MS (EI-MS) m/z calc. for $C_{22}H_{30}BrN_3O_2$ $(M+18)^+$ 466.41, found 466 and HR-MS (EI-MS) m/z calc. for $C_{22}H_{29}N_3O_2$ $(M-H-Br)^+$ 367.50, found 368.

2.3b *Compound 4-((3-formyl-4-hydroxyphenyl)azo)-1-dodecylpyridinium bromide (***2c***)*: Maroon solid. Yield: 90%; M.p.: 276–278 °C; IR (cm^{-1}): νOH 3391, $\nu CH_{aliphatic}$ 2925, 2854, νCH=O 2736, 2854, νC=O 1663, νN = N 1596, νC=C 1484, νC-O 1267; ^{1}H NMR (δ, ppm in DMSO-d6): 10.38–10.16 (s, 1H, C<u>H</u>=O), 8.67–8.64 (d, 2H), 8.04, 8.03 (d, 1H, *J*/Hz 2.28), 7.88, 7.87, 7.85, 7.84 (dd, 1H, ^{3}J/Hz 9.34, ^{5}J/Hz 2.19), 7.58-7.56 (d, 2H, *J*/Hz 5.89); 6.66-6.63 (d, 1H, *J*/Hz 9.30), 4.40–4.25 (t, 2H), 1.77–1.73 (m, 2H), 1.17 (bs, 18H); 0.80 (t, 3H); ^{13}C NMR (δ, ppm in DMSO-d6): 190.71, 183.37, 175.63, 162.35, 157.37, 151.49, 151.01,144.23, 141.62, 140.20, 131.30, 127.26, 126.33, 124.07, 123.52, 116.36, 115.92, 115.50, 32.27, 31.33, 29.05, 28.99, 28. 92, 28.76, 28.15, 27. 54, 22.14 and 13.97; HR-MS (EI-MS) m/z calc. for $C_{24}H_{34}BrN_3O_2$ $(M+H)^+$ 477.45, found 477.2 and HR-MS (EI-MS) m/z calc. for $C_{24}H_{33}N_3O_2$ $(M-H-Br)^+$ 395.54, found 396.

2.3c *Compound 4-((3-formyl-4-hydroxyphenyl)azo)-1-tetradecylpyridinium bromide (***2d***)*: Brown solid. Yield: 90%; M.p.: 288–289 °C; IR(cm^{-1}): νOH 3457, $\nu CH_{aliphatic}$ 2925, 2854, νCH=O 2736, 2854, νC=O 1663, νN=N 1599, νC=C 1481,νC-O 1267; ^{1}H NMR (δ, ppm in DMSO-d6): 10.43-10.19 (s, 1H, CHO), 8.78, 8.76 and 8.73, 8.71 (d, 2H, *J*/Hz 6.80); 8.18 and 8.03 (d, 1H), 8.10-8.05 and 7.92- 7.87 (dd, 1H); 7.83, 7.82 and 7.70, 7.69 (d, 2H, *J*/Hz 6.80), 7.13, 7.10 and 6.42, 6.39 (d, 1H, *J*/Hz 9.60), 4.42–4.38 (t, 2H); 1.90–1.80 (m, 2H), 1.4–1.1 (m, 22H); 0.86-0.82 (t, 3H), ^{13}C NMR (δ, ppm in DMSO-d6): 190.99, 183.35, 177.10, 162.35, 157.57, 151.00, 144.38, 141.65, 139.59, 133.12, 126.74, 126.37, 125.07, 123.66, 116.39, 115.46, 31.37, 30.66, 29.09, 28.87, 28.79, 28.49, 25.48, 22.17 and 14.01. HR-MS (EI-MS) m/z calc. for $C_{26}H_{38}BrN_3O_2$ $(M+H+18)^+$ 523.51, found 523.6 and HR-MS (EI-MS) m/z calc. for $C_{26}H_{37}N_3O_2$ $(M-H-Br)^+$ 423.59, found 423.4.

2.3d *Compound 4-((3-formyl-4-hydroxyphenyl)azo)-1-hexadecylpyridinium bromide (***2e***)*: Brown solid. Yield: 91%, M.p.: >300 °C; IR(cm^{-1}); νOH 3319, $\nu CH_{aliphatic}$ 2925, 2854, νCH=O 2736, 2854, νC=O 1670, νN=N 1596, νC=C 1483, νC-O 1271; ^{1}H NMR (δ, ppm in DMSO-d6): 10.38-10.07 (s, 1H, CHO), 8.69, 8.67 and 8.62, 8.60 (d, 2H, *J*/Hz 5.88 Hz), 8.00, 7.99 (d, 1H, *J*/Hz 2.7), 7.82, 7.81, 7.79, 7.78 (dd, 1H, ^{3}J/Hz 9.44, ^{5}J/Hz 2.71), 7.55, 7.53 (d, 2H, *J*/Hz 5.94); 6.52, 6.49 (d, 1H, *J*/Hz 9.45), 4.41-4.33 (t, 2H); 1.79–1.72 (m, 2H), 1.29–1.06 (m, 26H), 0.81–0.76 (t, 3H), ^{13}C NMR (δ, ppm in DMSO-d6): 191.04, 183.29, 178.06, 162.39, 157.58, 150.91, 144.27, 141.60, 139.17, 133.76, 126.50, 126.31, 125.49, 123.69, 116.39, 115.39, 31.30, 30.57, 29.05, 28.88, 28.78, 28.72, 28.40,

25.43, 22.10 and 13.95; HR-MS (EI-MS) m/z calc. for $C_{28}H_{42}BrN_3O_2$ $(M)^+$ 532.56, found 532 and HR-MS (EI-MS) m/z calc. for $C_{28}H_{41}N_3O_2$ $(M\text{-}H\text{-}Br)^+$ 451.65, found 452.

2.4 *Antibacterial activity*

The derivatives **2a–e** were screened for their antibacterial activity against *Bacillus cereus* (PTCC 1556), *Staphylococcus aureus* (PTCC 1112), *Escherichia coli* (PTCC 1330) and *Klebsiella pneumonia* (PTCC 1053) by the disc diffusion method.[20] Muller Hinton agar plates were inoculated with the 24 h cultures of bacteria. The synthesized derivatives were dissolved in DMSO and placed on the surface of the inoculated plates at the concentration of 30 μg/disc. Amikacin was used as the standard antibiotic. After incubation at 37 °C for 24 h, the diameter of inhibition zone was measured (mm). The minimum inhibitory concentration (MIC) values were also determined using the broth micro dilution method.[21]

2.5 *Free radical scavenging activity*

The free radical scavenging activity of the derivatives **2a–e** was determined using Diphenylpicrylhydrazyl (DPPH) method.[22] 50 μL of sample in DMSO (1 mg/mL) was mixed with 5 mL of DPPH (0.004% in methanol). The mixture was then vortexed vigorously and incubated in the dark at room temperature for 30 min. The absorbance was read at 517 nm against the blank. The radical scavenging activity (RSA) was calculated using the following formula:

$$\%\mathrm{RSA} = [(A_C - A_S)/A_C] \times 100 \quad (1)$$

Where, A_C is the absorbance of DPPH solution without sample as control and A_S is the absorbance of DPPH in the Presence of the sample. The results were compared to Ascorbic acid (Vitamin C) as standard. The IC_{50} value was calculated graphically based on the capacity of compound concentration to scavenge 50% of free radicals.

2.6 *Quantum chemical calculations*

The structural parameters of compounds evaluated by quantum chemical calculations using the Gaussian 03 program.[23] The gas phase geometries of **2a** were optimized using the DFT (B3LYP) method with the 6-311++G (2d, 2p) basis set. Harmonic frequency calculations were performed at all the stationary points to characterize its nature and to ensure that the optimized structure corresponds to a global minimum. The vibrational band assignments were made using the Gauss-View molecular visualization program.[24] Electronic excitations of the title compound were calculated by using TD-DFT for the gas phase.[25,26]

3. Results and Discussion

The azo pyridinium salts 4-((3-formyl-4-hydroxyphenyl)diazenyl-1-alkylpyridinium salts (**2a–e**) were prepared by the reaction of 2-hydroxy-5-(pyridine-4-yldiazenyl)benzaldehyde (**1**) with related n-alkyl bromides in ethanol (Figure 1a). Compounds **2a–e** are air-stable and soluble in THF, EtOH, CH_3CN, DMSO and DMF. The structures of **2a–e** were characterized by elemental analysis, mass, FT-IR, UV-Vis, ^1H and ^{13}C NMR spectroscopy. Compounds **2a–e** were tested for antibacterial and antioxidant properties.

3.1 *Spectral characterization*

The FT-IR spectra of **1** and **2a–e** are shown in supplementary information. After alkylation of **1**, two sharp peaks appeared in 2925 and 2854 cm^{-1} which correspond to the n-alkyl chain.

The ^1H NMR spectra of **2a–e** exhibited the C<u>H</u>=O proton signals at 10.19–10.07 ppm. The aromatic and aliphatic protons appeared at 8.75–6.38 ppm and 4.40–0.76 ppm, respectively. The ^{13}CNMR spectra of **2a–e** showed two peaks for carbonyl (191.20–190.71 and 183.37–182.96 ppm) and more than 10 peaks for aromatic carbons (178.06–115.39 ppm). The signals for the aliphatic carbons appeared at 45.74–13.95 ppm (Figures S2–S20 in Supplementary Information). Precise review of ^1H and ^{13}C NMR spectra showed that there is more than one structure in solution for **2a–e**. For example, in ^1H NMR spectrum for **2d**, there are three peaks for C<u>H</u>=O proton and the protons of pyridine ring in addition to the two doublets at 8.73–8.71 ppm and 7.83–7.81 ppm showed two doublets at 8.78–8.76 ppm and 7.70–7.69 ppm. The ortho proton to phenol group showed two separated doublets at 7.13–7.10 ppm and 6.42–6.39 ppm. Other weak bands are also observed in the ^1H NMR spectrum of **2d,** which clearly confirm the existence of three structures. Figure 1b displays three resonance structures for **2a–e** compounds. ^1H NMR spectrum of **2d** and the proposed structures are shown in Figure 2. In the ^{13}C NMR spectrum of **2d**, two peaks appeared at 190.99 and 183.35 ppm that can be attributed to the carbonyl group, which indicated there are two carbonyl groups in the solution (Figure S15, Supplementary Information). Accordingly, there are two or more structures for **2a–e** compounds which are due to the keto–enol tautomerism and hydrogen transfer. The ratio of resonance structures for **2a–e**, calculated by integral of C<u>H</u>=O in ^1H NMR spectra, is presented in Table 1. Also, to further explore the proposed structures, the ^1H NMR spectrum of **2d** was obtained by adding NaOH to the NMR tube. After the pH value was increased, the pertinent signals of

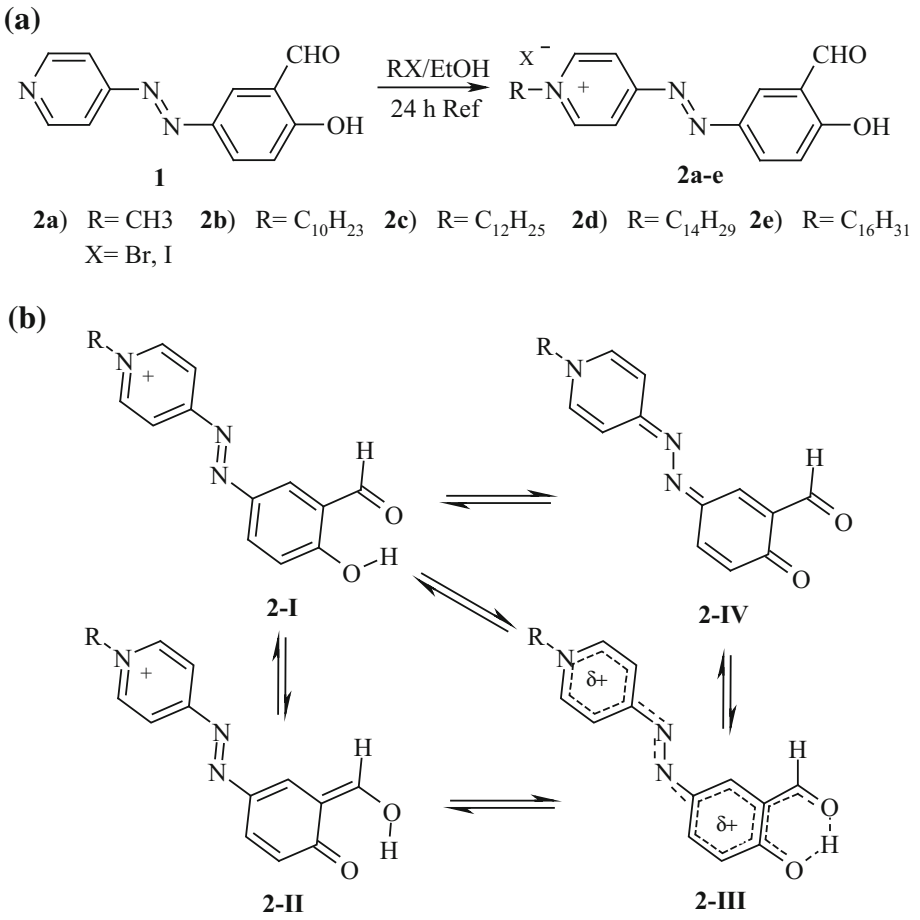

Figure 1. (a) The synthesis of compounds **2a–e**. (b) The proposed resonant structures for **2a–e**.

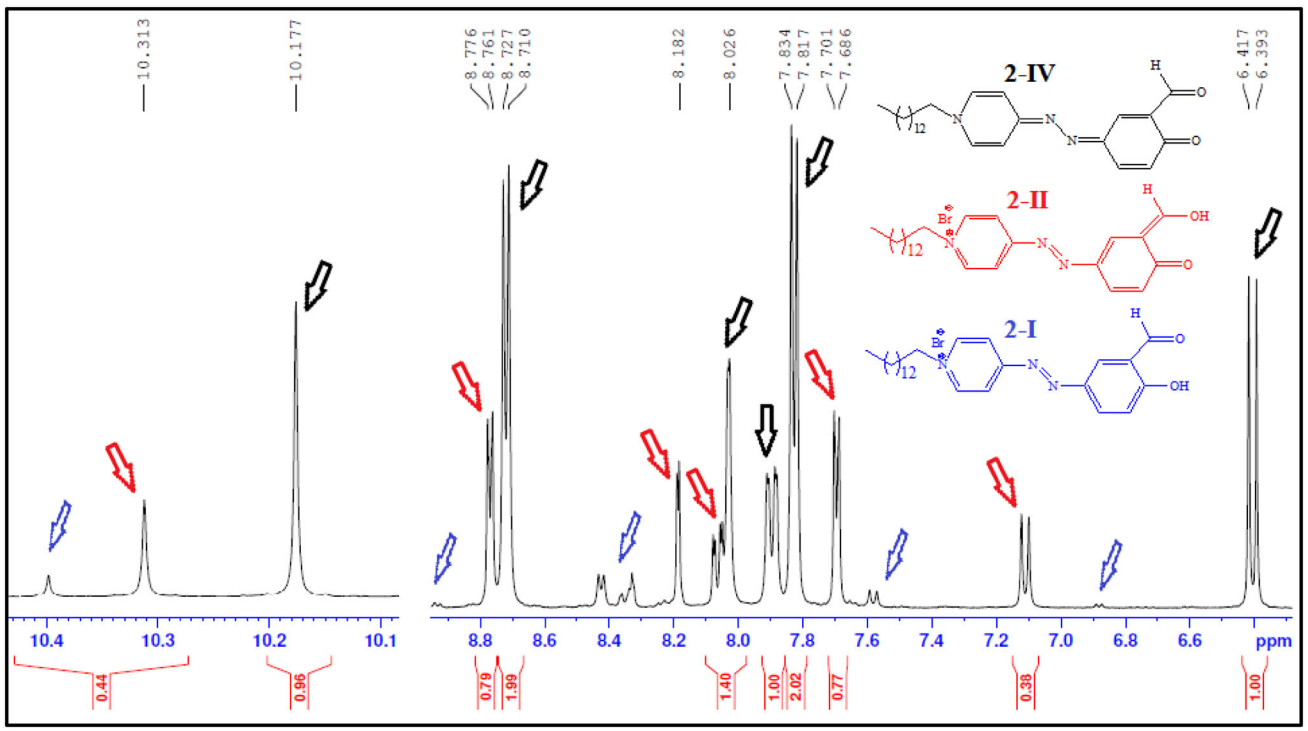

Figure 2. ^{1}H NMR Spectrum of **2d** (aromatic and aldehyde protons).

Table 1. The ratio of resonance structures in the DMSO (%).

Compound	**2-I** and **2-II**	**2-IV**
2a	37.28	62.72
2b	19.17	80.83
2c	22.26	77.74
2d	32.41	67.59
2e	18.15	81.15

2-IV structure did not change, while the related signals of **2-I** structure were deleted, and related signals to the **2-II** structure have been shifted toward **2-IV** signals. The shiftings are shown in Figure S14 (Supplementary Information) and attributed to partial dissociation of O–H bond at 2-II structure by adding the NaOH solution. The chemical structures are supported by UV-Vis spectra, as well.

3.2 *Electronic absorption spectroscopy*

The electronic absorption spectra of the synthesized compounds were recorded (in the range of 200–600 nm) in solvents DMSO, DMF, MeOH, and THF (2×10^{-5} M, 1 cm, quartz cell) at room temperature (Table 2). The UV-Vis absorption spectra of **1** show a band at 226–264 nm that is assigned to $\pi\rightarrow\pi^*$ transitions in the backbone of the aromatic ring. The second peak located at 349–422 nm is assigned to $\pi\rightarrow\pi^*$ electronic transition of the azo-aromatic chromophore. Furthermore, in the polar solvents of DMSO and DMF the third band at 450–481 nm is owing to $n\rightarrow\pi^*$ electronic transition of the azo-aromatic chromophore and intramolecular hydrogen bonding.[4,5]

The UV-Vis absorption spectra of **2a–e** in DMSO, DMF, MeOH, and THF solvents show a band at 219–268 nm that is assigned to $\pi\rightarrow\pi^*$ transitions in the backbone of the aromatic ring and displays bathochromic shift (positive solvatochromism) with polarity change of solvent. **2a–e** in MeOH and THF solvents show a band at 365–437 nm that is assigned to $\pi\rightarrow\pi^*$ electronic transition of azo–aromatic chromophore. In the DMSO and DMF solvents mainly two bands are displayed. The first band located at 385–405 nm is because of $\pi\rightarrow\pi^*$ transition of the aromatic ring while the second one at 475–486 nm is owing to intramolecular hydrogen bonding between the hydroxyl and carbonyl groups and it indicated the keto–enol tautomerism in compounds **2a–e** such as the whole of salicylaldehyde-based azo dyes.[19,27] The absorption spectra of **2d** in DMF, DMSO, THF, and MeOH with diverse salvation characters are shown in Figure 3a.

Table 2. Summary of the UV-Vis absorption bands for **1** and **2a–e** (nm).

Compound	DMSO	DMF	THF	MeOH
1	259, 406(sh), 480	264, 405(sh), 481	226, 422	248, 349,450 (Sh)
2a	251, 385, 475, 557	264, 394, 486(sh), 557	226, 367, 564	268, 365, 410(sh), 544
2b	256, 402(sh), 484, 556	270, 405(sh), 485, 555	222, 435, 567	248, 367,420(sh), 536
2c	254, 402(sh), 484, 556	270, 405(sh), 485, 558	219, 437, 567	248, 367,420(sh), 537
2d	254, 404(sh), 482, 556	270, 405(sh), 482, 558	220, 432, 567	251, 369,420(sh), 533
2e	255, 399(sh), 483, 556	270, 405(sh), 482, 555	219, 437, 567	248, 371,420(sh), 535

For **2a–e**, compared with **1,** there is an additional band at 533–567 nm in all of the solvents (Figures S21–S24 in Supplementary Information). The observed new peak is assumed to be associated with the development of appreciable **2-IV** conformer. This is in line with obtained results by ^{1}H, ^{13}C NMR and further confirmed by measuring the absorption properties in basic solutions. The absorption spectrum of **2d** was measured at different pH values (Figure S25 in Supplementary Information). As the pH value of the solution increased, the intensity of the band at 533–567 nm also increased. Dissociation of the phenolic proton results in the formation of **2-IV** tautomer. State "**2-IV**" is more favorable to form a conjugate structure than states "**2-I**" and "**2-II**". Therefore the longest red shift in the visible spectrum (533–567 nm) is observed for **2-IV**.[28] For further study about resonant structures; the Quantum chemical calculations were also done.

3.3 *Quantum chemical calculations*

To authenticate the electronic spectra of the compounds **2a–e**, TD-DFT calculations on electronic absorption spectra in the gas phase were performed. The maximum absorption peak (λ_{max}) in a UV-Vis spectrum corresponds to vertical excitation. TD-DFT calculations predict absorption bands with different UV-Vis regions for **2-III** and **2-IV** tautomers (Figure 3b). The absorption region of **2-IV** form is different than the **2-III**. It shows that **2-IV** has the longest wavelength of absorption in the electronic spectra. Hence, by comparing the calculated values of wavelengths with experimental data, it can be concluded that **2-IV** state could be the predominant tautomer in **2a–e** compounds in both solvent and gas phases (Figure 3 and Table 2).

The selected optimized geometric parameters for **2-III** and **2-IV** tautomers are listed in Table S1 for comparison (Figure S26) in Supplementary Information. There are some notable points in these results. In both structures, the torsion angles for N_{11}-N_{12}-C_{13}-C_{14}, C_6-N_{11}-N_{12}-C_{13}, C_5-C_6-N_{11}-N_{12}, and C_3-C_4-C_9-O_{10} are ca.180° or 0°. This indicates that the two aromatic rings and N=N and C=N bonds are planar and that it allows the π electron conjugation to extend throughout the aromatic rings.

The calculated stretching frequency of C=O and N=N bonds are found to be 1670–1780 cm^{-1} and 1520–1089 cm^{-1}, respectively, which agree with the experimental data (Table S1 and Figures S2–S5 in Supplementary Information). Furthermore, the $O_{10}\cdots H_1$ bond distance in the optimized structures of 2-III is 1.793 Å. This distance is shorter than the sum of van der Waals radii of oxygen (1.52 Å) and hydrogen (1.20 Å) atoms indicating the presence of hydrogen bonding interactions.

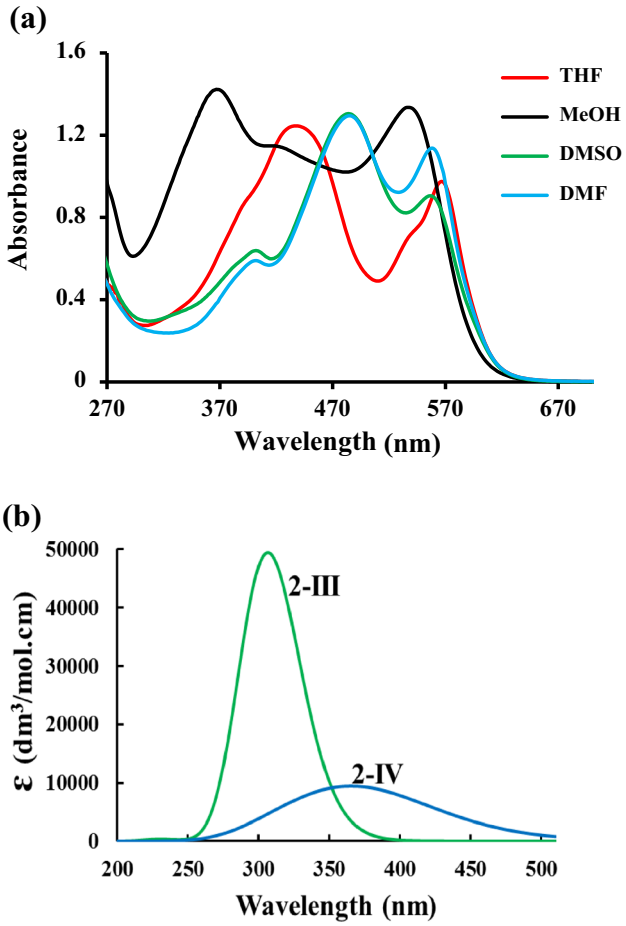

Figure 3. (a) Absorption spectra of **2d** in DMF, DMSO, MeOH and THF solvents (5×10^{-5} M, 1 cm, quartz cell). (b) The computed electronic spectra for **2-III** and **2-IV**.

3.4 *Biological activities*

Compounds **2a–e** were tested *in vitro* for antibacterial activity against *S. aureus*, *B. cereus*, *E. coli* and *K. pneumonia*. The results indicate that all of the prepared compounds had antibacterial activities against Gram-positive bacteria (*S. aureus* and *B. cereus*) (Figure 4), but they exhibited no activity against Gram-negative bacteria (*E. coli* and *K. pneumonia*). It is observed that compound **1** and **2a** show weak activity while **2b–e** display good activity against Gram-positive bacteria. These results show that the presence of the carbon chain is necessary to achieve antibacterial activity. Electrostatic interactions between the positively-charged QAC head and the negatively charged bacterial cellular membrane are followed by penetration of the side alkyl chains into the interface area disturb bacterial lipid bilayer membranes and leakage of the cellular content.[29] **2b** with

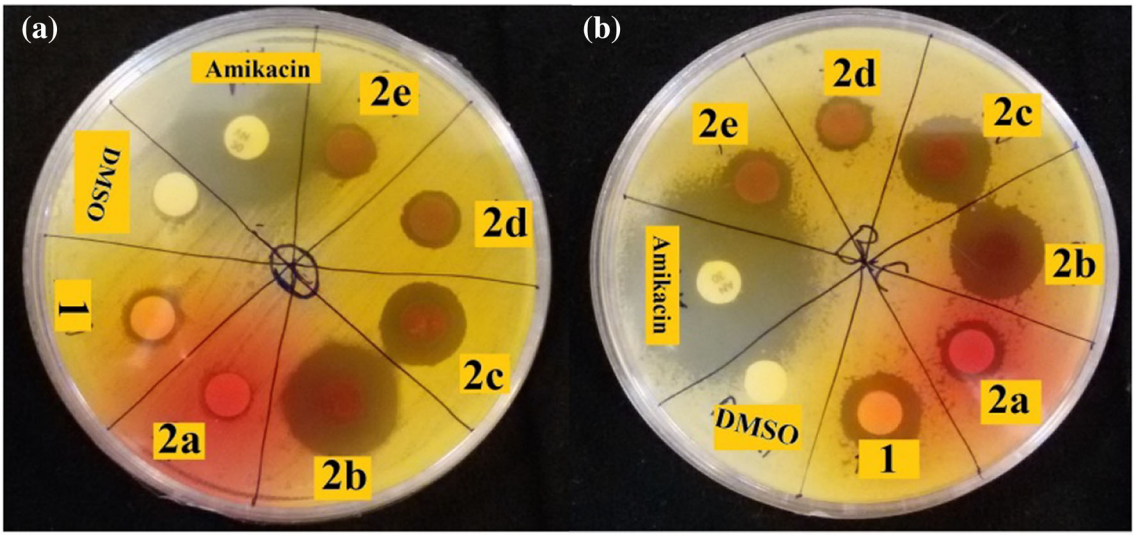

Figure 4. The antibacterial activity test against (a) *S. aureus* and (b) *B. cereus*.

Table 3. *In vitro* antimicrobial activities of synthesized compounds.

Compound (30 μg/disc)	Zone of inhibition (mm) against bacteria			
	S. aureus	*B. cereuss*	*E. coli*	*K. pneumonia*
1	8	10	–	–
2a	7	9	–	–
2b	17	14	–	–
2c	13	13	–	–
2d	9	9	–	–
2e	9	10	–	–
Amikacin	22	30	22	18

Table 4. Minimal inhibitory concentration of **2b** (μg/mL).

Compound	*S. aureus*	*B. cereuss*
2b	MIC (μg/mL)	
	31.2	62.5

decyl group displays the highest activity; the results are listed in Table 3.

Since compound **2b** shows the highest activity, it was further assessed to find minimal inhibitory concentration (MIC) against *S. aureus* and *B. cereus*, by broth macro-dilution method; the results are reported in Table 4.

Compounds **2a–e** were also evaluated for their scavenging activity by diphenyl picrylhydrazyl (DPPH) method. The results are presented in Table 5. A review of the data reveals that all azo pyridinium compounds show much better free radical inhibition compared to the corresponding azo ligand. The highest scavenger activity was observed in **2a**. Scavenging activity of all compounds was lower than the standard ascorbic acid with 97.04% activity. The 50% of inhibition values (IC_{50}) ranged from 1.58 to 9.28 mg/mL. **2a** showed the most potent activity with the IC_{50} value of 1.58 mg/mL; the results are listed in Table 6. It is reported that creation of the positive charge density by the formation of QACs improves the antioxidant properties.[30,31] Compounds **2a–e** have a hydroxyl group, and antioxidant activity can be strongly dependent on the position and number of hydroxyl groups due to the ability to produce active hydrogen.[32,33] It has been proposed that the scavenging activity may be associated to the reaction of DPPH-radical with active hydrogen and QACs as an electron-withdrawing group can reduce the dissociation energy of O–H and it facilitated the active hydrogen production.[34]

4. Conclusions

New alkyl pyridinium salts (**2a–e**) were prepared and characterized by various spectral techniques. The structural studies by UV-Vis and ^{1}H and ^{13}C NMR indicated keto–enol tautomerism with dipole moment changes

Table 5. Antioxidant activity of **1** and **2a–e** (%).

	DPPH Scavenging (%)						
Concentration 1000 (μg/mL)	**1**	**2a**	**2b**	**2c**	**2d**	**2e**	**Vitamin C**
	2.65	33.33	6.85	18.85	10.90	7.48	97.04

Table 6. The IC_{50} for antioxidant activity of **1** and **2a–e**.

Compounds (μg/mL)	IC_{50} (mg/mL)
1	19.25
2a	1.58
2b	9.28
2c	8.87
2d	6.66
2e	3.19
Vitamin C	0.05

in **2a–e** being dependent on the nature of solvent and pH. The NMR, UV-Vis absorption spectra and quantum chemical calculations of **2a–e** support a resonant structure compared to the azo precursor. The compounds **2a–e** show moderate-to-good antibacterial and antioxidant activity. The results show that the carbon chain is necessary to achieve antibacterial activity. The compounds **2b** and **2a** with decyl and methyl groups, respectively, exhibit the best antibacterial and antioxidant activity.

Supplementary Information (SI)

All additional information pertaining to experimental data and characterization of **1** and **2a–e** using FT-IR, UV-Vis, ^{1}H, ^{13}C and mass spectra are given in Figures S1–S25. The representative geometries of the optimized conformers of **2a** are given in S26; the list of the selected data for optimized structures of **2a** conformers are shown in Table S1. Supplementary Information is available at www.ias.ac.in/chemsci.

Acknowledgements

We are grateful to the Lorestan University for financial support of this work.

References

1. Merino E 2011 Synthesis of azobenzenes: The coloured pieces of molecular materials *Chem. Soc. Rev.* **40** 3835
2. Zollinger H 2003 In *Color Chemistry: Syntheses, Properties, and Applications of Organic Dyes and Pigments* (Weinheim: Wiley)
3. Zollinger H (Ed.) 1961 In *Azo and Diazo Chemistry: Aliphatic and Aromatic Compounds* (New York: Interscience publishers)
4. Ghasemian M, Kakanejadifard A, Azarbani F, Zabardasti A and Kakanejadifard S 2014 The triazine-based azo–azomethine dyes; spectroscopy, solvatochromism and biological properties of 2, 2′-((2, 2′-(6-methoxy-1, 3, 5-triazine-2, 4-diyl) bis (oxy) bis (2, 1-phenylene)) bis (azan-1-yl-1-ylidene) bis (methan-1-yl-1-ylidene)) bis (4-phenyldiazenyl) phenol *J. Mol. Liq.* **195** 35
5. Kakanejadifard A, Azarbani F, Zabardasti A, Kakanejadifard S, Ghasemian M, Esna-ashari F, Omidi S, Shirali S and Rafieefar M 2013 The synthesis, structural characterization and antibacterial properties of some 2-((4-amino-1, 2, 5-oxadiazol-3-ylimino) methyl)-4-(phenyldiazenyl) phenol *Dyes Pigments* **97** 215
6. Abuo-Melha H and Fadda A 2012 Synthesis, spectral characterization and in vitro antimicrobial activity of some new azopyridine derivatives *Spectrochim. Acta A* **89** 123
7. Vallabhajosula S 2011 Positron emission tomography radiopharmaceuticals for imaging brain beta-amyloid *Semin. Nucl. Med.* **4** 283
8. Marmion D M 1991 In *Handbook of US Colorants: Foods, Drugs, Cosmetics, and Medical Devices* (Weinheim: Wiley)
9. Kucharski T J, Ferralis N, Kolpak A M, Zheng J O, Nocera D G and Grossman J C 2014 Templated assembly of photoswitches significantly increases the energy-storage capacity of solar thermal fuels *Nat. Chem.* **6** 441
10. Gorostiza P and Isacoff E Y 2008 Optical switches for remote and noninvasive control of cell signaling *Science* **322** 395
11. Saphier S, Haft A and Margel S 2012 Bacterial reduction as means for colonic drug delivery: Can other chemical groups provide an alternative to the azo bond? *J. Med. Chem.* **55** 10781
12. Towns A 1999 Developments in azo disperse dyes derived from heterocyclic *Diazo Compon.* **42** 3
13. Seferoglu Z and Ertan N 2007 Synthesis and spectral properties of new hetarylazo indole dyes Russian *J. Org. Chem.* **43** 1035
14. Zelenitsky S A and Zhanel G G 1995 Phenazopyridine in urinary tract infections *Ann. Pharmacother.* **30** 866
15. Merianos J J 1991 Quarternary ammonium antimicrobial compound. In *Disinfection, Sterilization and Preservation*, 4th edn. (Philadelphia: Lea & Feiber) p. 225
16. Yadav P, Kumar B, Gautam H K and Sharma S K 2017 Synthesis and antibacterial activity screening of quaternary ammonium derivatives of triazolyl pyranochromenones *J. Chem. Sci.* **129** 211
17. Rhein L 1997 In vitro interactions: biochemical and biophysical effects of surfactantson skin In *Surfactants in Cosmetics* 2nd edn. Martin Reiger (Ed.) (New York: Routledge) Ch. 18

18. Shelton R, Campen M v, Tilford C, Lang H, Nisonger L, Bandelin F and Rubenkoenig H 1946 Quaternary ammonium salts as germicides. I. Non-acylated quaternary ammonium salts derived from aliphatic amines1 *J. Am. Chem. Soc.* **68** 753
19. Odabaşoğlu M, Albayrak Ç, Özkanca R, Aykan F Z and Lonecke P 2007 Some polyhydroxy azo–azomethine derivatives of salicylaldehyde: Synthesis, characterization, spectroscopic, molecular structure and antimicrobial activity studies *J. Mol. Struct*. **840** 71
20. Bauer A, Kirby W, Sherris J C and Turck M 1966 Antibiotic susceptibility testing by a standardized single disk method *Am. J. Clin. Pathol.* **45** 493
21. Jorgensen J H 1993 Methods for dilution antimicrobial susceptibility tests for bacteria that grow aerobically: Approved standard: NCCLS document M7-A3 Nccls
22. Shimada K, Fujikawa K, Yahara K and Nakamura T 1992 Antioxidative properties of xanthan on the autoxidation of soybean oil in cyclodextrin emulsion *J. Agric. Food Chem*. **40** 945
23. Frisch M, Trucks G, Schlegel H, Scuseria G, Robb M, Cheeseman J, Montgomery Jr J, Vreven T, Kudin K and Burant J 2004 Gaussian 03, revision c. 02 (Wallingford, CT: Gaussian. Inc.)
24. Dennington R, Keith T, Millam J, Eppinnett K, Hovell W L and Gilliland R 2009 *GaussView* (Shawnee Mission: Semichem Inc)
25. Runge E and Gross E K 1984 Density-functional theory for time-dependent systems *Phys. Rev. Lett.* **52** 997
26. Bauernschmitt R and Ahlrichs R 1996 Treatment of electronic excitations within the adiabatic approximation of time dependent density functional theory *Chem. Phys. Lett.* **256** 454
27. Zakerhamidi M, Nejati K, Sorkhabi S G and Saati M 2013 Substituent and solvent effects on the spectroscopic properties and dipole moments of hydroxyl benzaldehyde azo dye and related Schiff bases *J. Mol. Liq.* **180** 225
28. Xia W, Huang C, Ye X, Luo C, Gan L and Liu Z 1996 Photochromic and electrochemical properties of a Novel Azo pyridinium compound and its Langmuir–Blodgett films *J. Phys. Chem.* **100** 2244
29. Denyer S P 1995 Mechanisms of action of antibacterial biocides *Int. Biodeter. Biodegr.* **36** 227
30. Luan F, Wei L, Zhang J, Tan W, Chen Y, Dong F, Li Q and Guo Z 2018 Preparation and characterization of quaternized chitosan derivatives and assessment of their antioxidant activity *Molecules* **23** 516
31. Liu J, Sun, H, Dong F, Xue Q, Wang G, Qin S and Guo Z 2009 The influence of the cation of quaternized chitosans on antioxidant activity *Carbohydr. Polym.* **78** 439
32. Abdel-Aziz M, Abuo-Rahma G E-D A and Hassan A A 2009 Synthesis of novel pyrazole derivatives and evaluation of their antidepressant and anticonvulsant activities *Eur. J. Med. Chem.* **44** 3480
33. Özil M, Parlak C and Baltaş N 2018 A simple and efficient synthesis of benzimidazoles containing piperazine or morpholine skeleton at C-6 position as glucosidase inhibitors with antioxidant activity *Bioorg. Chem.* **76** 468
34. Chen T, Xu P, Zong S, Wang Y, Su N and Ye M 2017 Purification, structural features, antioxidant and moisture-preserving activities of an exopolysaccharide from Lachnum YM262 *Bioorg. Med. Chem. Lett.* **27** 1225